

Quantum effects on the structure of pure and binary metallic nanoclusters

R. Ferrando,¹ A. Fortunelli,^{2,*} and G. Rossi¹

¹*INFN and IMEM/CNR, Dipartimento di Fisica, Via Dodecaneso 33, Genova, I16146, Italy*

²*Molecular Modeling Laboratory, IPCF/CNR, Via G. Moruzzi 1, Pisa, I56124, Italy*

(Received 26 April 2005; published 24 August 2005)

A family of high-symmetry bimetallic clusters—recently shown to give rise to “magic” structures in the case of Ag-Cu and Ag-Ni nanoclusters—is investigated also in the case of Ag-Pd, Ag-Co, Au-Cu, Au-Ni, and Au-Co. Cluster structures obtained by global optimization within a semiempirical potential model are then reoptimized via density functional calculations. Sizes up to 45 atoms are considered. Ag-Cu, Ag-Ni, and Au-Ni clusters have some common characteristics. They present polyicosahedral character and achieve maximum stability at the Ag- and Au-rich compositions, when the structural arrangement is associated to a Ni(Cu)core-Ag(Au)shell chemical ordering. This is due both to the huge size mismatch between the components and a clear tendency of the larger atoms to segregate at the surface. In Au-Cu and Ag-Pd, clusters achieve their best stability at intermediate compositions, in agreement with the tendency of these metals to mix in the bulk phase. Finally, for Ag-Co and Au-Co, peculiar quantum effects favor intermediate compositions despite the fact that these metal phases separate in the bulk. These results are rationalized in terms of the interplay between electronic and volumetric effects on the structure of metallic nanoclusters.

DOI: [10.1103/PhysRevB.72.085449](https://doi.org/10.1103/PhysRevB.72.085449)

PACS number(s): 61.46.+w, 73.22.-f, 31.10.+z

I. INTRODUCTION

Bimetallic nanoclusters have recently attracted increasing interest for their peculiar catalytic, optical, magnetic, electric, and mechanical properties.^{1,2} Especially intriguing is the possibility of finely tuning the properties of nanoclusters not only by varying their size, but also their composition. Bimetallic catalysts are important in a number of practical processes, including automobile exhaust conversion and petroleum naphtha reforming. One of the major problems which arises in the study of these systems is their structural characterization, a prerequisite for a deeper understanding and modeling of their properties. In this respect, theoretical approaches can give a useful contribution by restricting the search to few structural candidates. However, the determination of the most favorable structures of bimetallic clusters is a formidable task, due to the huge amount of combinatorial possibilities which exponentially complicates the theoretical prediction.³ Particular importance is then assumed by the study of those structures which possess high energetic stability, that might serve as building blocks for cluster-assembled materials.

In a previous work,⁴ a family of polyicosahedral structures has been described, and has been shown to give rise to “magic” clusters (i.e., clusters of remarkable structural, electronic and thermodynamic stability) for Ag-Cu and Ag-Ni bimetallic particles with a low fraction of Cu or Ni occupying the interior of a core-shell arrangement. The structural stability of these core-shell clusters was rationalized in terms of (a) reduction of internal and surface bond strain with respect to pure clusters due to the size mismatch between the larger Ag atom and the smaller Cu and Ni atoms, (b) smaller Ag surface energy which favors segregation of the Ag atoms at the surface. These factors cause the remarkable stability of the (27,7) [and also (30,8) and (32,6)] “magic” polyicosahedral clusters.

As the pairs gold/silver and cobalt/nickel have similar radii, it is worthwhile investigating whether these findings can

be extended to the Ag-Co, Ag-Pd, Au-Cu, Au-Ni, and Au-Co combinations. In the present paper density functional (DF) calculations are employed to study these systems. Our results confirm the strong tendency of small bimetallic clusters to alloying.⁴ For all systems considered here, even for those that present a very strong tendency against mixing in the bulk phase, mixed cluster are energetically more favorable than pure ones.

In addition, we find that subtle quantum effects can modulate this propensity giving rise to interesting variations. The behavior of Au-Ni is similar to the behavior of Ag-Cu and Ag-Ni, namely with a tendency to favor core-shell polyicosahedral structures, as indicated by both formation and excess energies which have lower values for Au-rich compositions (corresponding to the Ni-core–Au-shell arrangement). On the other hand, Au-Cu clusters do not single out the core-shell arrangement as being especially favorable, since formation energies are almost constant for compositions extending from the Au-rich to the Cu-rich side. This is consistent with the tendency of Au-Cu to mix in the bulk phase, forming a series of ordered alloys. Also for Ag-Pd both Ag-rich and intermediate compositions present low excess energies, and a clear tendency to form polyicosahedral structures. Finally, for Ag-Co and Au-Co we show that magnetic effects destabilize the core-shell arrangement. In this case, polyicosahedral structures are again very stable, but peculiar quantum effects bring the minimum in the formation energies from Au- or Ag-rich to intermediate compositions, presenting a much more thorough intermixing of the two atoms. This behavior is at variance with the tendency of Ag-Co and Au-Co to separate in the bulk phase, and is peculiar of finite or confined systems (see, for example, the observation of alloyed Ag-Co thin films on crystal surfaces⁵). Band structure and shell-closure effects on the geometries of pure metallic clusters are also found.

In Sec. II we briefly sketch the computational method. In Sec. III we describe polyicosahedral clusters and define the

quantities which are used to characterize the energetic stability of mixed clusters. Sections IV and V are devoted to the results. Before dealing with mixed systems, in Sec. IV we consider the pure clusters whose properties serve as a starting point for studying mixed clusters. Section V reports the results about mixed systems. Finally, Sec. VI contains the discussion and conclusions.

II. COMPUTATIONAL METHOD

The density functional calculations are carried out with the DF module of the NWChem package (release 4.5),⁷ and use the Becke functional⁸ for exchange and the Perdew-Wang functional⁹ for correlation. $(7s6p6d)/[5s3p2d]$ Gaussian-type-orbital basis sets and effective core potentials are used for all elements, derived from Refs. 10 and 11 for Ag and Ref. 12 for Cu, Ni, and Co, and modified combining the suggestions in <ftp://ftp.chemie.uni-karlsruhe.de/pub/basen> and Ref. 13. Charge density fitting $(11s4p5d3f4g)/[11s4p4d3f2g]$ Gaussian-type-orbital basis sets were used to compute the Coulomb potential.¹⁴ All the calculations have been performed spin-unrestricted, and using a Gaussian-smearing technique¹⁵ for the fractional occupation of the one-electron energy levels, which improved the self-consistent convergence process, ensured that the final spin state was a local minimum in the spin space, avoided symmetry-breaking issues for Jahn-Teller systems, and did not affect the value of the energy as in almost all cases the one-electron energy gap was larger than the chosen smearing parameter $\sigma=0.02$ eV. A numerical grid of 65 radial points and 350 points for the angular part was used for evaluating the exchange-correlation potential and energy. The geometry optimization was stopped when the numerical force on atoms was less than 4×10^{-4} a.u. More details on the numerical procedure can be found in Ref. 13.

The initial configurations for DFT relaxation are provided by a genetic global-optimization procedure⁴ unless otherwise specified.

III. STRUCTURAL FAMILIES AND ENERGETIC STABILITY INDEXES

The structures which are considered in the present work are depicted in Figs. 1–3. In particular, we focus attention on polyicosahedral (pIh) clusters, which are built by packing elementary icosahedra (Ih) of 13 atoms as described in Ref. 4. In the following, a pIh of size N , made of N_1 Ag or Au (large) atoms and $N_2=N-N_1$ Cu, Ni, Pd or Co (small) atoms, and comprising m interpenetrating Ih_{13} will be referred to as $(N_1, N_2)\text{pIh}^m$. These structures are very compact and exhibit a large number of bonds. However, inner atoms have nearest-neighbor distances which are very compressed with respect to the nearest-neighbor distance between surface atoms, so that these configurations are not favored in pure clusters. They become very competitive when their internal core is substituted with metal atoms of a smaller size, due to the combined effect of decrease in strain and the surface segregation of the metal with lower surface energy. Interestingly, the $(27,7)\text{pIh}^7$ structure—which in Ref. 4 resulted to be the

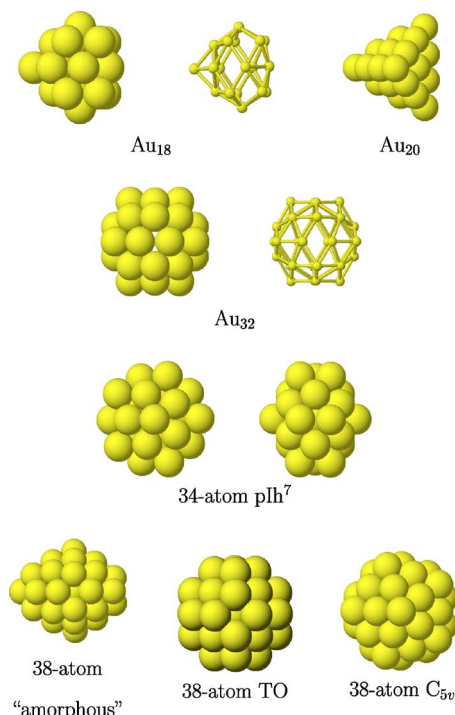


FIG. 1. (Color online) Schematic pictures of pure metallic clusters considered in this work.

stablest in the pIh family—has first been found as the lowest-energy isomer of pure Al₃₄,⁶ in this case the pIh structure is favored by the presence of a second minimum in the interaction potential at roughly the second-neighbor distance. As we shall see in the following also high-stability cage-like structures (which are found in gold clusters) are closely related to polyicosahedral structures.

Other structures of importance for clusters in this size range are the following. First of all, the truncated octahedron (TO) of 38 atoms (TO₃₈), which is simply a piece of fcc bulk

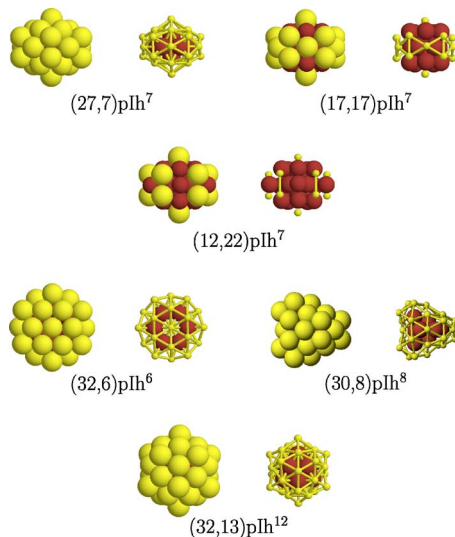


FIG. 2. (Color online) Schematic pictures of mixed bimetallic clusters considered in this work. Light grey atoms are either Ag or Au, whereas darker atoms are either Cu, Ni, Pd, or Co.

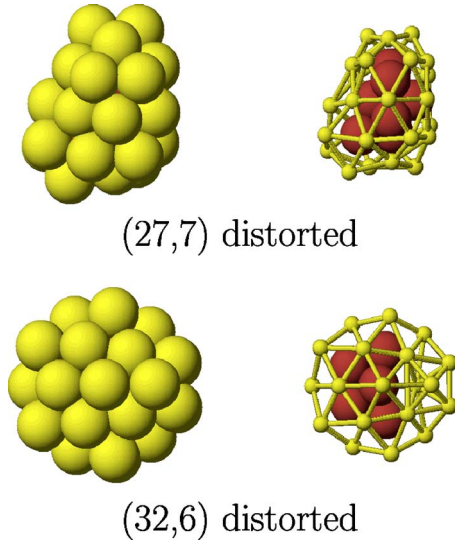


FIG. 3. (Color online) Schematic pictures of mixed bimetallic clusters considered in this work. Here the distorted structures are shown for the case Ag-Cu. Light grey atoms are either Ag, whereas darker atoms are Cu.

lattice and is a putative global minimum for silver, copper, and nickel clusters according to semiempirical potential calculations.^{4,16} Then, the low-symmetry cluster of size 38, which is a putative global minimum for gold.¹⁷ Finally, another cluster of size 38 which is obtained as a fragment of the icosahedron of 55 atoms. This fragment has C_{5v} symmetry group, and, according to semiempirical potential calculations,¹⁸ is the second isomer for both Ag and Cu, being however quite close in energy to the TO_{38} .

The criterion that we use for comparing the relative stability of clusters with a different number of atoms is the excess energy with respect to N bulk atoms, divided by $N^{2/3}$,

$$\Delta = \frac{E_{DF}^{N_1, N_2} - N_1 \varepsilon_1^{\text{coh}} - N_2 \varepsilon_2^{\text{coh}}}{N^{2/3}}, \quad (1)$$

where N_1 and $\varepsilon_1^{\text{coh}}$ are the number and the bulk cohesive energy of one metallic species, whereas $N_2 = N - N_1$ and $\varepsilon_2^{\text{coh}}$ are the same quantities for the other metallic species, and $E_{DF}^{N_1, N_2}$ is the DF binding energy for the given cluster, identified by its size and composition. Stable structures are identified by low Δ values. For the cohesive energies we take the experimental values (in eV), $\varepsilon_{\text{Cu}}^{\text{coh}} = 3.50$, $\varepsilon_{\text{Ag}}^{\text{coh}} = 2.95$, $\varepsilon_{\text{Au}}^{\text{coh}} = 3.82$, $\varepsilon_{\text{Ni}}^{\text{coh}} = 4.47$, $\varepsilon_{\text{Co}}^{\text{coh}} = 4.45$, $\varepsilon_{\text{Pd}}^{\text{coh}} = 3.89$. Δ is the excess energy divided by $N^{2/3}$. $N^{2/3}$ is roughly proportional to the number of surface atoms in the cluster.

However, Δ may be a biased quantity when comparing clusters of the same size but different compositions. For example, as we shall see in the following, pure gold clusters present large Δ , whereas pure copper clusters have much lower Δ . This means that when comparing Au-Cu clusters, those with Au-rich compositions will present larger Δ . To avoid this bias, we use also other energetic stability indexes, Δ_{34} and Δ_{38} , defined in such a way that their value for pure clusters is zero (or small anyway) for sizes 34 and 38, respectively. Let us consider, for example, Δ_{38} . At this size, we

consider pure TO_{38} clusters of the two species 1 and 2, and calculate their binding energies per atom $\varepsilon_1(TO_{38})$ and $\varepsilon_2(TO_{38})$. Then we define Δ_{38} as

$$\Delta_{38} = E_{DF}^{N_1, N_2} - N_1 \varepsilon_1(TO_{38}) - N_2 \varepsilon_2(TO_{38}), \quad (2)$$

Δ_{34} is defined in the same way, but taking the energies per atom of pure 34-atom pIh⁷ clusters. Clusters with negative values of Δ_{34} or Δ_{38} are energetically favored over the 34-atom pIh⁷ or the TO_{38} . The physical meaning of Δ_{34} and Δ_{38} is easy to understand, they represent the energy gain (or loss) for a mixed cluster with respect to pure clusters of size 38 or 34. Therefore Δ_{34} and Δ_{38} are the equivalent, in the case of nanoclusters, of the formation energy of bulk alloys.

IV. RESULTS FOR PURE CLUSTERS

Let us start by analyzing the DF results for pure clusters in Table I, whose schematic pictures are shown in Fig. 1. The first noteworthy point is that the truncated octahedron configuration is not the lowest-energy one for pure coinage-metal M_{38} clusters. This is the first indication that quantum (in this case, band structure) effects can be important for medium-size clusters. The scheme of the one-electron energy levels is in fact very similar for Cu_{38} , Ag_{38} , and Au_{38} , and is such that they are not closed-shell systems, the majority-spin HOMO is degenerate and partially filled (Jahn-Teller systems). This non-shell-closure effect destabilizes the TO configuration, and because of that a lower energy is achieved with lower-symmetry isomers. However, there is a difference between Cu and Ag on the one hand and Au on the other hand. In fact the TO Au_{38} cluster is predicted to be at a higher energy with respect to a low-symmetry isomer (see Fig. 1) also using atom-atom potentials,^{16,17} an example of amorphization of small clusters due to the increased “bond-stickiness” of the gold atom with respect to Cu and Ag atoms,¹⁹ whereas the TO Cu_{38} and Ag_{38} clusters are predicted to be the lowest energy configurations by atom-atom potentials,^{16,18} so that their being at a higher energy (even though by small amounts) with respect to a lower-symmetry isomer (essentially, a fragment of the Ih_{55} of C_{5v} symmetry group, which is also a capped decahedron with atomic islands on anti-Mackay stacking,²⁰ see Fig. 1) is an unexpected result due to a purely electronic effect.

Electronic effects are important also at size 34. At this size, the pure M_{34} pIh⁷ configurations (see Fig. 1) have a lower Δ with respect to the TO_{38} for Cu and Ag, but a higher Δ for Au, due to the fact that pIh structures have very compressed internal bonds, and are thus highly disfavored in the case of “sticky” metals such as gold, which present in addition a very strong bond-order–bond-length correlation^{21,22} as a further destabilizing factor for pIh structures. This trend about the energetic stability of M_{34} pIh⁷ structures in coinage metals is thus in agreement with the predictions based on semiempirical potential modeling.^{19,20}

This analysis, based on the interplay between electronic and ionic effects, can be further deepened by observing that $N=34$ is a magic number for the spherical hard-wall jellium electronic model.²³ In fact, an analysis of the one-electron spectrum of pure and mixed coinage metal $N=34$ clusters

TABLE I. DF calculations results for pure clusters. Values of spin (S), HOMO-LUMO energy difference (gap, in eV) for alpha/beta electrons, and excess energy (Δ , in eV) with respect to N bulk atoms, see Eq. (1). The symbol “JT” after the gap value signals a Jahn-Teller system, with a degenerate HOMO (symmetry breaking is not allowed during the DF relaxation in these cases).

System	Size	Structure	S	Gap	Δ	Δ_{38}	Δ_{34}
Cu	34	pIh ⁷	0	0.88	4.20	0.51	0.00
	38	TO	1	0.61/0.56 JT	4.30	0.00	-0.12
	38	C _{5v}	0	0.34	4.29	-0.09	-0.21
Ag	34	pIh ⁷	0	0.91	3.99	3.28	0.00
	38	TO	1	0.39/0.35 JT	4.06	0.00	-3.63
	38	C _{5v}	0	0.43	4.03	-0.28	-3.91
Au	18	C _{2v} (cage)	0	1.38	5.02	2.18	-0.02
	20	Td	0	2.10	5.02	0.97	-1.47
	32	Ih(cage)	0	1.78	5.55	-1.69	-5.60
	34	pIh ⁷	0	0.79	6.22	4.05	0.00
	38	TO	1	0.12/0.08 JT	6.05	0.00	-4.66
	38	“amorphous”	0	0.19	5.97	-0.92	-5.58
Ni	34	pIh ⁷	13.2	0.10/0.04 JT	5.09	2.29	0.00
	38	TO	16	0.21/0.03 JT	5.08	0.00	-2.59
Co	34	pIh ⁷	31	0.12/0.08 JT	5.39	2.56	0.00
	38	TO	32	0.43/0.08 JT	5.34	0.00	-3.28
Pd	38	TO	4	0.17/0.10	4.07	0.00	

shows that the s component can be described as a $1s1p1d2s1f$ jellium sequence. The shell-closure effects account for the large HOMO-LUMO gaps for all those clusters for size 34. Also the peculiar stability of the 34-atom mixed clusters, and especially of the (27,7)pIh⁷ arrangement in the case of Ag-Cu, Ag-Ni, and Au-Ni (see the next section and Ref. 4) is partly attributable to this effect. Because of the electronic shell closure, Cu₃₄ and Ag₃₄ have a relatively low Δ , despite the fact that internal bonds are very compressed in pIh arrangements of pure clusters. In the case of Au₃₄, atom-atom interactions are more sticky, and the bond-order–bond-length correlation is stronger than in Ag and Cu. Therefore, the internal strain in Au₃₄ is too high, and the cluster has a large excess energy.

Internal strain in pure Au polyicosahedra is so high that cagelike structures can become competitive, and as an example in Table I we report an Au₃₂ cluster. This cluster is an Ih cage (see Fig. 1), corresponding to the external skeleton of the (32,13)pIh¹² bimetallic anti-Mackay icosahedron (Fig. 2, see Ref. 4 and the following section) which has recently been shown²⁴ to possess remarkable stability. An analysis of the one-electron spectrum of Ih Au₃₂ reveals that its s component can be well described as a $1s1p1d1f$ jellium sequence (one s shell of the spherical layered hard-wall jellium model is destabilized by the inner void). The analogous Ih Ag₃₂ cagelike cluster is not favored because the larger spatial extent of the $5s$ orbital produces a destructive interference.

In this connection, one can predict for gold a very stable shell closing at $N=18$, corresponding to the $1s1p1d$ jellium sequence. In fact we were able to find a C_{2v} cagelike structure at $N=18$ (see Fig. 1) with a very low excess energy

(especially considering that Δ usually increases with decreasing the size of the cluster), see Table I. This 18-atom cage has been found by genetic optimization of a cluster of size 20, made of 18 gold atoms and two copper atoms within a semiempirical potential modeling. This optimization has produced a core-shell structure with the two copper atoms inside, and a gold shell outside. After removing the copper atoms, the resulting gold shell has been relaxed by DF calculations.

Finally, it can be noted that the stability of the tetrahedral Au₂₀ cluster²⁵ (which is reported for comparison in Table I and Fig. 1) can be explained by a shell closing effect within a tight-binding analysis framework.²⁶

V. RESULTS FOR BINARY CLUSTERS

A. Ag- X clusters

The DF results for Ag-containing clusters are given in Table II. Here we consider four systems, Ag-Cu, Ag-Ni, Ag-Pd, and Ag-Co. First, we discuss Ag-Cu and Ag-Ni (in comparison with Ag-Pd), and then we focus on Ag-Co that presents a peculiar behavior.

1. Ag-Cu, Ag-Ni, and Ag-Pd

For Ag-Cu and Ag-Ni clusters of size 34, the excess energy as a function of the first-row transition metal composition has a minimum for the (27,7)pIh⁷ structure (called five-fold pancake in the following), a minimum which is appreciably lower than the excess energy of the pure species.⁴ In the Ag-Cu case, we have also locally optimized

TABLE II. DF calculations results for Ag-containing clusters. Values of spin (S), HOMO-LUMO energy difference (gap, in eV) for alpha/beta electrons, and excess energy (Δ , in eV) with respect to N bulk atoms, see Eq. (1). The symbol “JT” after the gap value signals a Jahn-Teller system, with a degenerate HOMO (symmetry breaking is not allowed during the DF relaxation in these cases).

System	Size	Structure	S	Gap	Δ	Δ_{38}	Δ_{34}
Ag-Cu	34	(27,7)pIh ⁷	0	0.82	3.68	-2.88	-5.55
	34	(27,7)distorted	0	0.24	3.77	-1.97	-4.47
	34	(17,17)pIh ⁷	0	0.94	3.80	-2.39	-4.00
	34	(12,22)pIh ⁷	0	0.88	3.90	-1.70	-2.84
	38	(32,6)pIh ⁶	0	0.34	3.90	-2.21	-5.26
	38	(32,6)distorted	0	0.18	3.87	-2.59	-5.64
	38	(30,8)pIh ⁸	0	0.26	3.80	-3.50	-6.35
	45	(32,13)pIh ¹²	2.5	0.49/1.00	3.98	-8.95	-13.03
Ag-Ni	34	(27,7)pIh ⁷	3.5	0.81/0.46	3.74	-3.93	-4.36
	34	(17,17)pIh ⁷	6.5	0.19/0.07	4.22	-1.99	-3.11
	34	(12,22)pIh ⁷	7	0.26/0.07 JT	4.49	-0.60	-2.07
	38	(32,6)pIh ⁶	0	0.09	4.00	-2.47	-5.76
	38	(30,8)pIh ⁸	0	0.05	3.92	-3.99	-7.18
	45	(32,13)pIh ¹²	4	0.59/0.06 JT	3.96	-8.23	-11.89
Ag-Co	34	(27,7)pIh ⁷	0	0.22	4.10	-0.64	-3.63
	34	(17,17)pIh ⁷	17	0.95/0.13 JT	4.38	-1.57	-4.53
	38	(32,6)pIh ⁶	6	0.36/0.22	4.10	-1.76	-5.09
	45	(32,13)pIh ¹²	10.5	0.80/0.31	4.12	-7.11	-11.03
Ag-Pd	38	(32,6)pIh ⁶	0	0.14	3.80	-2.97	
	38	(26,12)pIh ⁶	0	0.14	3.76	-3.45	

the energy of a (27,7) low-symmetry isomer, taking as starting structure the one predicted as the second isomer by a semiempirical atom-atom potential (for technical details, see Ref. 4), the corresponding result is reported as a 34-atom distorted cluster in Table II and depicted in Fig. 3. This low-symmetry isomer lies at 0.8 eV above the pIh structure, thus confirming the remarkable (magic) stability of this arrangement. The additional stability of the $N=34$ configuration due to the previously discussed jellium shell-closure effect also plays a role in favoring polyicosahedral structures. In the case of Ag-Cu, 34-atom polyicosahedra present large HOMO-LUMO gaps for all compositions. Shell-closure effects producing pronounced stability have been previously described in small bimetallic clusters, see, for example, Refs. 29–31. In the case of Ag-Pd, size mismatch is not large enough to stabilize the fivefold pancake according to the atom-atom potential, and therefore we have not considered this cluster.

Let us now consider size 38. Composition (32,6) is interesting for the competition of different possible structures. The global optimization by atom-atom potential⁴ for this composition gives the (32,6)pIh⁶ structure (called in the following sixfold pancake) as the global minimum for Ag-Cu, Ag-Ni, Ag-Pd and also in Au-Cu.^{27,28} For Ag-Pd the same structure is found also for a wide range of compositions, extending to (20,18). Comparing fivefold and sixfold pancake structures, it can be noted that the sixfold pancake maximizes the number of mixed bonds, while the fivefold

pancake has a compact nucleus of small atoms. Moreover, the fivefold pancake prefers a huge size mismatch, while the sixfold pancake prefers a somewhat smaller size mismatch. As a result, in systems such as Ag-Cu and Ag-Ni, which present huge size mismatch and no preferential tendency for making mixed bonds, there is a whole family of structures of size 38 which have close resemblance with the fivefold pancake, and that are in competition with the sixfold pancake already at the atom-atom potential level. After DF relaxation, one of these structures (the distorted cluster of size 38, see Fig. 3) becomes lower in energy than the sixfold pancake in Ag-Cu. In Ag-Pd, such distorted structure is completely unfavorable because the size mismatch is too small, and the two metals have a better tendency to form mixed bonds. Finally, in Au-Cu, there is both a strong tendency to form mixed bonds and a large size mismatch. These two features act in opposite direction on the stability of the sixfold pancake, so that it is not easy to understand whether this structure can retain the global minimum also at the DF level. This point is currently under investigation.

However, in agreement with the atom-atom calculations,⁴ for Ag-Cu and Ag-Ni at size 38, the structure with the most favorable energetic stability indexes is not found at composition (32,6) but at composition (30,8). Here we find the (30,8)pIh⁸, which is the perfect core-shell polyicosahedron with the largest Ni or Cu core. For Ag-Pd, the energetic stability indexes are favorable for a series of sixfold pancakes of different compositions. In agreement with the atom-

atom potential calculations, and with the tendency of Ag and Pd to mix, the (26,12)pIh⁶ (which is not a core-shell structure, but presents an intermediate Pd layer) is more favorable than the core-shell (32,6)pIh⁶.

2. Ag-Co

The results for the Ag-Co system present some peculiarity. Here we have not performed atom-atom global optimization, but simply taken the same structures of Ag-Cu and Ag-Ni and performed DF relaxation, in order to compare the same structures for different systems. From Tables I and II, we can see that Δ at size 34 is increasing from pure silver ($\Delta=3.99$) to pure cobalt ($\Delta=5.39$), without giving a preference for the clusters of intermediate composition. However, since Δ values for pure Ag and Co clusters differ significantly, it is better to consider the unbiased indicators Δ_{34} and Δ_{38} . Both Δ_{34} and Δ_{38} are negative for mixed Ag-Co clusters, confirming the general trend of nanoalloy clusters to a negative formation energy, even in systems where the bulk formation energy is positive. However, at variance with Ag-Cu and Ag-Ni, which present the most negative Δ_{34} and Δ_{38} in correspondence with perfect core-shell clusters (that is for silver-rich compositions), Ag-Co clusters present values of Δ_{34} and Δ_{38} which are smaller in absolute value and moreover reach their minimum for intermediate compositions. This indicates a somewhat reduced chemical interaction and a more pronounced tendency towards intermixing of Ag-Co with respect to Ag-Ni and Ag-Cu (see also the behavior of Au-Cu and Au-Co in the next section for comparison). Before discussing the origin of this behavior, we note that we even found severe convergence problems in the self-consistent process for the (30, 8)pIh⁸ and (12,22)pIh⁷ clusters, so that the corresponding results are not reported in Table II.

What is the origin of the different behavior of Ag-Co compared to Ag-Ni and Ag-Cu?

Ni and Co have very similar atomic radii, and the Ag-Co bulk phase diagram is similar to the Ag-Ni (and also Ag-Cu) phase diagram.³² All these binary systems present a very limited miscibility in the bulk phase. However, magnetic effects are appreciably more important in Co than in Ni. It can be reminded, for example, that bulk Co has an hcp structure—at variance with the other metals considered in this work, which present an fcc structure in the bulk.

In this connection, it is instructive to analyze the DF-optimized geometries of pure M₃₈ TO structures, reported in Table III. From this analysis, it can be seen that pure Cu₃₈ and Ag₃₈ TO clusters essentially correspond to a section of the fcc crystal, apart from a slight outward protrusion of the atoms on the (111) faces.³³ This protrusion is essentially due to the bond-order–bond-length correlation in metallic systems,^{21,22} and quantitatively predicted by atom-atom potentials.³⁴ This outward protrusion is very pronounced in the Au₃₈ TO, which is a sign of strong bond-directionality effects in gold clusters,³⁵ similar to those found for platinum clusters in Refs. 13 and 36. A completely analogous behavior to Cu₃₈ and Ag₃₈ is present in the Ni₃₈ TO cluster, except that now the whole structure is “shrunk” by a larger factor with respect to the crystal. For the Co₃₈ TO cluster, instead, the

TABLE III. Values of geometrical parameters for M₃₈ truncated octahedral (TO) clusters from DF calculations. In a TO cluster, one has an inner shell atom (I) surrounded by an outer shell composed of vertex (IIv) and (111) face (IIIf) atoms. The values refer to representative atoms in the upper half of the cluster as ratios of Cartesian coordinates over the absolute value of the y coordinate of the IIv atoms (the D₄ axis of the cluster coincides with the z axis). The ratio of y_{IIv} with its “ideal” crystal value is also given. For a cluster which is a section of an “ideal” fcc lattice, these values should read 1.0, 2.0, 1.0, 1.0.

System	z_I/y_{IIv}	z_{IIv}/y_{IIv}	z_{IIIf}/y_{IIv}	$y_{IIv}^{\text{crystal}}/y_{IIv}$
Co ₃₈	1.05	1.99	1.00	0.975
Ni ₃₈	1.01	2.01	1.03	0.976
Cu ₃₈	1.01	1.99	1.03	0.992
Ag ₃₈	1.00	2.00	1.03	0.998
Au ₃₈	0.99	1.99	1.08	0.996
Pt ₃₈	0.99	1.99	1.09	0.987

(111) faces become completely “flat,” whereas the internal octahedral atoms expand by $\approx 4\%$, thus hinting at being in a “coordinatively unsaturated” situation. This thus suggests that the buried Co atoms in the core-shell pIh structures are less stable than the corresponding Ni or Cu atoms because of unfavorable magnetic interactions. This interpretation is supported by analysis of the DF-optimized (27,7)pIh⁷ Ag₂₇Co₇ structure, which shows a large structural relaxation of the internal Co atoms. In fact, a comparison between the pIh⁷ Ag₂₇Co₇ and Ag₂₇Ni₇ structures shows that the Ag external cage is practically unaltered in the two clusters (with differences in the interatomic distances of the order of 0.3%), whereas the Co atoms at the apexes of the fivefold bipyramid shrink their distance by $\approx 5.5\%$. In parallel, the electron spin is quenched to $S=0$, and the gap in the one-electron energy spectrum drops from 0.81/0.46 eV to 0.22 eV.

B. Au-X clusters

The DF results for Au-containing clusters are given in Table IV. For Au-X clusters, we have preferred to relax (by DF calculations) the same structures that we found in Ag-Cu and Ag-Ni, instead of performing an independent global optimization by means of an atom-atom potential. However we remark that the core-shell polyicosahedra considered for Au-rich composition are indeed the global minima of the atom-atom potential in Au-Cu.²⁷

Since pure gold clusters present a much larger excess energy than pure clusters of the other metals considered here,³⁷ it is better to consider Δ_{34} and Δ_{38} to discuss the energetic trends at fixed size and varying composition. In passing, we note that we found convergence problems in the self-consistent process for the (30,8)pIh⁸ Au-Ni and Au-Co clusters, so that the corresponding results are not reported in Table IV.

The main outcome of these calculations is that (a) for Au-X clusters Δ_{34} and Δ_{38} show negative formation energies for any composition considered here, as found for Ag-X, but larger in absolute values. (b) The lowest value Δ_{34} and Δ_{38} is

TABLE IV. DF calculations results for Au-containing clusters. Values of spin (S), HOMO-LUMO energy difference (gap, in eV) for alpha/beta electrons, and excess energy (Δ , in eV) with respect to N bulk atoms, see Eq. (1). The symbol “JT” after the gap value signals a Jahn-Teller system, with a degenerate HOMO (symmetry breaking is not allowed during the DF relaxation in these cases).

System	Size	Structure	S	Gap	Δ	Δ_{38}	Δ_{34}
Au-Cu	34	(27,7)pIh ⁷	0	0.97	4.85	-6.65	-9.86
	34	(17,17)pIh ⁷	0	0.75	4.31	-7.13	-9.20
	34	(12,22)pIh ⁷	0	1.06	4.12	-6.58	-8.04
	38	(32,6)pIh ⁶	0	0.30	5.18	-6.78	-10.90
	38	(30,8)pIh ⁸	0	0.37	5.03	-7.39	-11.05
	45	(32,13)pIh ¹²	2.5	0.40/0.63	5.16	-8.95	-13.03
Au-Ni	34	(27,7)pIh ⁷	3.5	0.98/0.24	4.90	-7.04	-10.79
	34	(17,17)pIh ⁷	6.5	0.63/0.16	4.73	-6.71	-9.92
	34	(12,22)pIh ⁷	9	0.30/0.08 JT	4.79	-4.56	-7.51
	38	(32,6)pIh ⁶	3	0.28/0.05 JT	5.33	-6.43	-10.70
	45	(32,13)pIh ¹²	1	0.48/0.17 JT	5.19	-11.64	-16.37
Au-Co	34	(27,7)pIh ⁷	4	0.32/0.37	5.20	-5.11	-8.97
	34	(17,17)pIh ⁷	17	0.66/0.13 JT	4.80	-7.24	-10.93
	34	(12,22)pIh ⁷	22	0.95/0.17	4.81	-6.01	-9.32
	38	(32,6)pIh ⁶	6	0.29/0.29	5.38	-6.43	-10.70
	45	(32,13)pIh ¹²	10.5	0.45/0.33	5.26	-11.73	-16.69

obtained for gold-rich compositions in the case of Au-Ni clusters (see the results at size 34), so that the core-shell polyicosahedral structure is singled out as being of special stability, in analogy with Ag-Cu and Ag-Ni. However, in Ag-Ni, the tendency to favor core-shell polyicosahedra is stronger than in Au-Ni. (c) For Au-Cu, one finds that the three mixed compositions considered here give clusters of substantially comparable stability—with the preferred composition depending on the choice of the stability index (Δ , Δ_{34} , or Δ_{38}). (d) For Au-Co, the results are analogous to Ag-Co, with a preference for the intermediate composition, which is remarkable due to the tendency of Au and Co to phase separation in the bulk. However, formation energies are much more negative in Au-Co than in Ag-Co.

The following facts can help rationalize these findings.

As a general remark, chemical bonding effects play a more important role for Au than for Ag,³⁵ due to the more substantial contribution of the d orbitals to bonding (directionality effects³⁸) and the smaller spatial extent of the s orbitals, which strengthens the Au chemical interaction with first-row transition metals such as Cu, Ni, and Co. This explains the larger absolute values of Δ_{34} and Δ_{38} for Au- X clusters with respect to Ag- X clusters.

Moreover, the Au-Cu bulk phase diagram is different from those of the Au-Ni, Au-Co, and Ag- X systems.³² While the latter in fact show a very limited miscibility of the two components, the Au-Cu phase diagram presents three stable ordered alloys at compositions Au₃Cu, AuCu, and AuCu₃, with a larger melting temperature for the two phases with larger Cu concentration. This helps explaining point (c), i.e., the fact that in the Au-Cu case the cluster stability is substantially flat as a function of Au concentration. Also the somewhat larger surface energy of Au with respect to Cu (Refs. 39

and 40) contributes to disfavoring the segregation of a complete layer of Au to the surface.

In order to explain the somewhat weaker tendency of Au-Ni in favor of core-shell polyicosahedra with respect to Ag-Ni, it can be observed that—despite the fact that Au and Ag have very similar atomic radii—gold is a “stickier” metal than silver, and one in which directionality (chemical bonding) effects play a very important role.³⁵ These factors are against core-shell polyicosahedral structures (as seen already for pure Au clusters), and in principle could destabilize them. However, the driving forces towards core-shell polyicosahedra are so strong that these destabilizing factors eventually have a rather weak effect, which has some quantitative relevance but does not induce qualitative changes.

Au-Co clusters favor intermediate compositions as in Ag-Co. However, in the case of the (27,7) Au-Co clusters, the peculiar internal relaxation of the internal Co atoms is not taking place as in Ag-Co, and the spin is not quenched to zero. This explains why the values of Δ_{34} and Δ_{38} are much more negative than in Ag-Co.

Finally we remark that also 34-atom polyicosahedral Au-Cu clusters present large HOMO-LUMO gaps, due to the electronic shell-closing effect predicted by the hard-wall jellium model.

VI. CONCLUSIONS

A family of polyicosahedral bimetallic core-shell nano-clusters, recently shown to possess peculiar structural, thermodynamic, and electronic (“magic”) stability in the case of the Ag-Cu and Ag-Ni nanoalloys,⁴ has been investigated in the case of Ag-Pd, Ag-Co, Au-Cu, Au-Ni, and Au-Co via first-principles (DF) calculations.

The tendency of these structures to being “magic” has been rationalized in terms of general arguments considering the interplay of surface energy, size mismatch and bond-order–bond-length correlation.

On the basis of these general arguments, one would make the following predictions. The polyicosahedral core-shell arrangement should be especially favorable in those systems presenting size mismatch and tendency to phase separation in the bulk phase, with the large atoms segregating at the surface. These features are found in Ag-Co, Au-Ni, and Au-Co, besides the already studied⁴ Ag-Cu and Ag-Ni. By contrast, Ag-Pd and Au-Cu tend to mix in bulk phases, so that intermixed clusters (obtained at intermediate compositions) as well as core-shell clusters (obtained at silver-rich composition for Ag-Pd and gold-rich compositions for Au-Cu) could be favored.

The DF results confirm the validity of the general arguments for Ag-Cu, Ag-Ni, Ag-Pd, Au-Ni, and Au-Cu, while in clusters containing cobalt, peculiar quantum effects cause a qualitatively different behavior.

In the case of Ag-Co, the interaction among the magnetic moments of the buried Co atoms oppose the gain in energy associated with the shrinking of the cluster size and the reduced strain. In the case of Au-Co, the latter effect is less evident, but chemical bonding effects (connected with the strong directionality of the Au-Au bonding³⁵) combined with the “sticky” character of the Au-Au interaction¹⁹ moves the maximum in the stability of the bimetallic clusters as a function of concentration from structures with a perfect core-shell arrangement to configurations with a substantial intermixing of the two atoms. Unfavorable magnetic interactions also contribute to destabilize Ni₃₄ and Co₃₄ clusters.

Apart from magnetic and chemical bonding effects, interesting electronic effects are also found for pure clusters.

In particular, band structure effects are found to disfavor “crystalline” (TO) arrangements in pure Cu₃₈ and Ag₃₈ clusters, nonsymmetrical structures (actually, defected decahedral M₅₅ configurations) which appear as closely competing low-lying isomers from atom-atom calculations are predicted to be at lower energy from first-principles calculations, essentially because the TO clusters are found to be Jahn-Teller systems and, as such, not particularly favored.

This non-shell-closure effect can be contrasted with the additional stability imparted to $N=34$ pure and bimetallic clusters by shell closing within the spherical hard-wall jellium model, to Au₁₈ or Au₃₂ clusters within the spherical layered hard-wall jellium model, and to Au₂₀ within a tight-binding approach. In general, a large value of the HOMO-LUMO gap is a signature of a shell-closure effect, which—in the case of gold—is amplified by the smaller extent and stronger interaction of the electronic wave function with respect to the Ag case.

We conclude by remarking that our results confirm the strong tendency of small bimetallic clusters to mixing,⁴ for all systems considered here, even for those that present a very strong tendency against mixing in the bulk phase (such as Ag-Cu, Ag-Ni, Ag-Co, or Au-Co), mixed cluster are characterized by large negative values of formation energy (Δ_{34} and Δ_{38} in Tables II and IV). This can be understood in terms of the greater structural freedom which reduced symmetry systems (such as clusters and surfaces) possess with respect to the constraints due to translational invariance of pre-defined lattices in bulk systems. For example, this structural freedom helps nanoclusters in accommodating strain in size-mismatched systems.

Quantum effects are found to often reinforce the tendency to mixing. They are particularly important for nanoclusters (in general, confined systems) with respect to bulk systems due to the neater separation between electronic shells, and the reduction in interatomic distances due to bond-order–bond-length correlation, which strengthens chemical bonding.

ACKNOWLEDGMENTS

The authors acknowledge financial support from the Italian CNR for the project “(Supra-)Self-Assemblies of Transition Metal Nanoclusters” within the framework of the ESF EURO-CORES SONS, and from European Community Sixth Framework Programme for the project “Growth and Supra-Organization of Transition and Noble Metal Nanoclusters” (Contract No. NMP4-CT-2004-001594). One of the authors (A. F.) acknowledges the Italian INSTM for a grant at the CINECA supercomputing center (Bologna, Italy).

*Corresponding author. Electronic address: fortunelli@ipcf.cnr.it

¹*Progress in Experimental and Theoretical Studies of Clusters*, edited by T. Kondow and F. Mafuné (World Scientific, New York, 2003).

²K. J. Klabunde, *Free Atoms, Clusters and Nanoscale Particles* (Academic, New York, 1994); K. J. Klabunde, *Nanoscale Materials in Chemistry* (Wiley, New York, 2001).

³J. Jellinek and E. B. Krissinel, “Alloy clusters: Structural classes, mixing, and phase changes,” in *Theory of Atomic and Molecular Clusters with a Glimpse at Experiments*, edited by J. Jellinek (Springer, Heidelberg, 1999).

⁴G. Rossi, A. Rapallo, C. Mottet, A. Fortunelli, F. Baletto, and R. Ferrando, *Phys. Rev. Lett.* **93**, 105503 (2004).

⁵G. E. Thayer, V. Ozolins, A. K. Schmid, N. C. Bartelt, M. Asta, J. J. Hoyt, S. Chiang, and R. Q. Hwang, *Phys. Rev. Lett.* **86**, 660 (2001).

⁶J. P. K. Doye, *J. Chem. Phys.* **119**, 1136 (2003).

⁷R. A. Kendall, E. Aprà, D. E. Bernholdt, E. J. Bylaska, M. Dupuis, G. I. Fann, R. J. Harrison, J. Ju, J. A. Nichols, J. Nieplocha, T. P. Straatsma, T. L. Windus, and A. T. Wong, *Comput. Phys. Commun.* **128**, 260 (2000).

⁸A. D. Becke, *Phys. Rev. A* **38**, 3098 (1988).

⁹J. P. Perdew, J. A. Chevary, S. H. Vosko, K. A. Jackson, M. R. Pederson, D. J. Singh, and C. Fiolhais, *Phys. Rev. B* **46**, 6671 (1992).

¹⁰A. Schaefer, C. Huber, and R. Ahlrichs, *J. Chem. Phys.* **100**,

- 5289 (1994).
- ¹¹D. Andrae, U. Haeussermann, M. Dolg, H. Stoll, and H. Preuss, *Theor. Chim. Acta* **77**, 123 (1990).
- ¹²M. Dolg, U. Wedig, H. Stoll, and H. Preuss, *J. Chem. Phys.* **86**, 866 (1987).
- ¹³E. Aprà and A. Fortunelli, *J. Phys. Chem.* **107**, 2934 (2003).
- ¹⁴Courtesy of Dr. Florian Weigend, Karlsruhe, Germany.
- ¹⁵C. Elsässer, M. Fähnle, C. T. Chan, and K. M. Ho, *Phys. Rev. B* **49**, 13975 (1994); R. W. Warren and B. I. Dunlap, *Chem. Phys. Lett.* **262**, 384 (1996).
- ¹⁶K. Michaelian, N. Rendón, and I. L. Garzón, *Phys. Rev. B* **60**, 2000 (1999).
- ¹⁷I. L. Garzon, K. Michaelian, M. R. Beltran, A. Posada-Amarillas, P. Ordejon, E. Artacho, D. Sanchez-Portal, and J. M. Soler, *Phys. Rev. Lett.* **81**, 1600 (1998).
- ¹⁸F. Baletto, A. Rapallo, G. Rossi, and R. Ferrando, *Phys. Rev. B* **69**, 235421 (2004).
- ¹⁹F. Baletto, R. Ferrando, A. Fortunelli, F. Montalenti, and C. Motet, *J. Chem. Phys.* **116**, 3856 (2002).
- ²⁰F. Baletto and R. Ferrando, *Rev. Mod. Phys.* **77**, 371 (2005).
- ²¹J. M. Soler, M. R. Beltrán, K. Michaelian, I. L. Garzón, P. Ordejon, D. Sánchez-Portal, and E. Artacho, *Phys. Rev. B* **61**, 5771 (2000).
- ²²J. M. Soler, I. L. Garzón, and J. D. Joannopoulos, *Solid State Commun.* **117**, 621 (2001).
- ²³M. Manninen, "Models of metal clusters and quantum dots," in *Atomic Clusters and Nanoparticles*, NATO ASI Les Houches LXXIII, edited by C. Guet, P. Hobza, F. Spiegelman, and F. David (Springer, Berlin, 2000).
- ²⁴X. Gu, M. Ji, S. H. Wei, and X. G. Gong, *Phys. Rev. B* **70**, 205401 (2004).
- ²⁵J. Li, X. Li, H.-J. Zhai, and L.-S. Wang, *Science* **299**, 864 (2003).
- ²⁶A. Fortunelli (unpublished).
- ²⁷A. Rapallo, G. Rossi, R. Ferrando, A. Fortunelli, B. C. Curley, G. M. Tarbuck, L. D. Lloyd, and R. L. Johnston, *J. Chem. Phys.* **122**, 194308 (2005).
- ²⁸G. Rossi, R. Ferrando, A. Rapallo, A. Fortunelli, B. C. Curley, L. D. Lloyd, and R. L. Johnston, *J. Chem. Phys.* **122**, 194309 (2005).
- ²⁹U. Heiz, A. Vayloyan, and E. Schumacher, *J. Phys. Chem.* **100**, 15033 (1996).
- ³⁰M. Heinebrodt, N. Malinoski, F. Tast, W. Branz, I. M. L. Billas, and T. P. Martin, *J. Chem. Phys.* **110**, 9915 (1999).
- ³¹E. Janssens, H. Tanaka, S. Neukermans, R. E. Silverans, and H. Lievens, *New J. Phys.* **5**, 46.1 (2003).
- ³²R. Hultgren, P. D. Deai, D. T. Hawkins, M. Gleiser, and K. K. Kelley, *Values of the Thermodynamic Properties of Binary Alloys* (American Society for Metals, Berkeley, 1981).
- ³³E. Aprà and A. Fortunelli, *J. Mol. Struct.: THEOCHEM* **501/502**, 251 (2000).
- ³⁴V. Rosato, M. Guillopé, and B. Legrand, *Philos. Mag. A* **59**, 321 (1989).
- ³⁵A. Fortunelli and A. M. Velasco, *Int. J. Quantum Chem.* **97**, 654 (2004).
- ³⁶E. Aprà, F. Baletto, R. Ferrando, and A. Fortunelli, *Phys. Rev. Lett.* **93**, 065502 (2004).
- ³⁷Due to basis set limitations and especially to the fact that the quality of the DF approach is not homogeneous for all the metals, experimental bulk binding energies have been taken as a reference for evaluating Δ .
- ³⁸S. Taylor, G. W. Lemire, Y. M. Hamrick, Z. Fu, and M. D. Morse, *J. Chem. Phys.* **89**, 5517 (1988).
- ³⁹W. R. Tyson and W. A. Miller, *Surf. Sci.* **62**, 267 (1977).
- ⁴⁰A. R. Miedema, *Z. Metallkd.* **69**, 287 (1978).